Traversing and labeling interconnected vascular tree structures from 3D medical images

Walter O'Dell[1], S. Tirumalai Govindarajan[3], Ankit Salgia, Satya Hedge[2], Sreekala Prabhakaran[2], Ender A. Finol[4], R. James White[5]

Departments of Radiation Oncology[1] and Pediatrics[2], University of Florida, Gainesville, FL
[3]A. Martinos Center for Biomedical Imaging, MGH, Boston, Mass; [4]Department of Biomedical Engineering, University of Texas, San Antonio, San Antonio, TX
[5]Department of Medicine, Pulmonary Diseases and Critical Care, University of Rochester Medical Center, School of Medicine and Dentistry, Rochester, NY

I. INTRODUCTION

Detailed characterization of vascular anatomy has important applications for the diagnosis and management of a variety of vascular diseases. Of particular impartance to our groups are vascular changes in response to radiation exposure[1], remodeling in response to chronic pulmonary arterial hyptertension[2], and lung vascular development in children born extremely preterm[3]. Improved characterization of the vascular tree structure would impact clinical decision-making, assessment of therapeutic efficacy, and evaluation of novel therapies. More accurate quantification of the vascular tree structure would also enhance our ability to understand the biological and biomechanical[4] underpinnings of these diseases and the sequelae of events that lead to disease progression and patient death. Much prior effort has led to successsful means to extract, segment and quantify vascular tree structures from 3D medical images to gather information on the number or branches, number of bifurcations, and branch length and volume[5].

However, to-date, little emphasis has been made on the accurate traversal of vessel trees that exhibit erroneous interconnections between adjacent trees. The use of large through-plane voxel dimensions and patient motion during imaging result in neighboring vessels that blur into the same voxel, thereby making them appear to be contiguous in the image set. This poster presents strategies and parameters used to traverse complicated vessel trees from a manually-selected seed point located near the root, where the algorithm identifies and repairs false-apparent tree connections to provide a more accurate representation of branch number and generation while isolating individual tree structures from amongst a complex intermingling of trees. A series of two-dimensional (2D) virtual datasets with a variety of interconnections were constructed for development, testing, and validation.
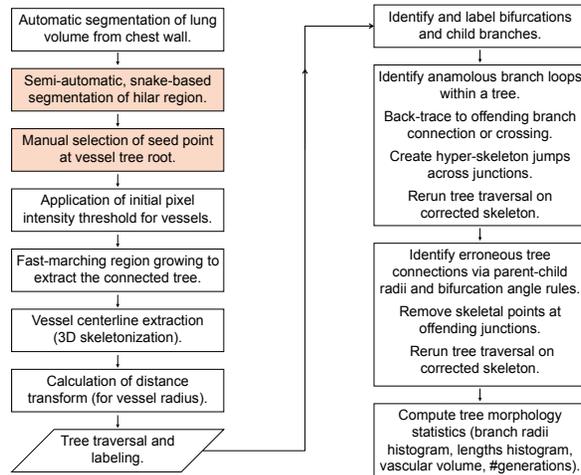
II. METHODS

Figure 1. Flow diagram of the semi-automated lung and vessel tree-segmentation procedure. The right column depicts the traversal and labeling algorithm. The procedure is fully automated except at the blocks marked with orange background. The semi-automatic, snake-based segmentation of the pediatric dataset shown in Fig 4. (241 slices) took ~40 minutes. The rest of the processing took < 8 minutes running on a MacPro with 12 CPUs (at 2.66 GHz) and 14 GB of RAM.
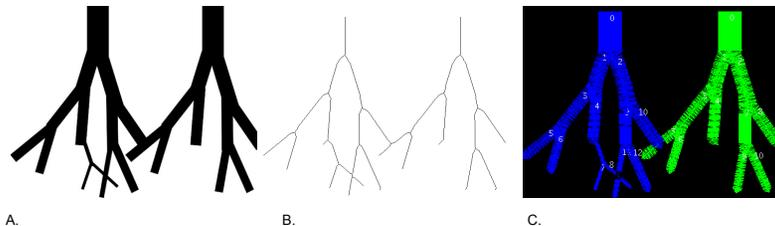

Figure 2. Validation on 2D virtual phantom. Figure A shows a 2D phantom exhibiting multiple branches, a crossing branch pair, and an anomalous connection between 2 trees. Figure B shows the initial 2D skeleton of the full structure. Figure C shows the output of our algorithm where each tree is given a unique color and there are hyper-skeleton jumps at crossings.
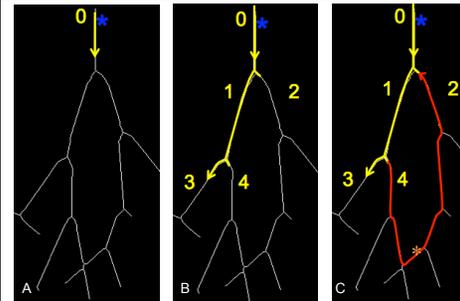
III. RESULTS

Figure 3. [A] Image A depicts the user-selected seed point (blue asterisk) and initial downward traversal for the crossing tree shown in Figure 2B (flipped left-right for clarity). **[B]** Image B depicts the initial labeling of child branches as the traversal encounters 2 bifurcation points, where the first point of each child is recorded prior to traversal down one of the child branches. **[C]** Image C depicts the eventual state where the traversal through the descendants of branch 4 encounters an anomalous crossing and begins traversing backwards up the tree. The traversal ultimately encounters the branch point that is already associated with branch 2. The tree is then retraced from the looped-to branch (2) to identify where the anomalous crossing occurred (indicated here by the orange asterisk).
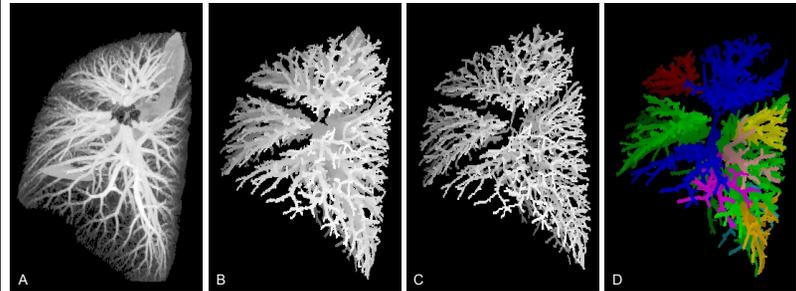

Figure 4. Application to a healthy adult human contrast-enhanced chest CT data set. **[A]** Image A is a maximum intensity projection (MIP) of the CT dataset of the right hemi-lung after extraction of the lung volume. This is a side view of the chest looking outward from the perspective of the heart with the lung apex at the top. **[B]** Image B is a depth-enhanced MIP of the extracted vessel tree structure resulting from a region-growing algorithm seeded at the root of one of the large vessels in the lower right hemi-lung. The distinct vascular beds of the 3 right lung lobes are apparent in this view. **[C]** Image C is a depth-enhanced MIP of the skeletonized tree in the same orientation. **[D]** Image D is a colorized MIP of the simulated image of the 8 largest vessel trees resulting from the splitting of each connected tree. The initial vessel extraction step identified 2,660 branches, with an incorrect estimate of 200 branch generations. After correcting for erroneous connections between adjacent trees, the corrected tree structure was found to have 1,960 branches on 32 independent trees.

IV. CONCLUSIONS/FUTURE WORK

We have introduced a set of schemata to extract, traverse, and label complex vascular tree structures that identifies and corrects anomalous branch connections arising from partial volume artifacts and other artifacts inherent in medical image datasets. This approach has been validated in complex 2D test cases and applied to *in vivo* human CT datasets, a CT scan of an anthropomorphic chest phantom, and a micro-CT dataset from an excised rat lobe. This work represents the first successful approach to distinguishing individual vascular trees from among a complex intermingling of trees and is expected to improve our ability to characterize changes in the vascular structure in disease and in response to therapy

V. REFERENCES

1. O'Dell WG, Wang P, *et al*. In-vivo Quantification of Human Lung Dose Response Relationship. *Proc. SPIE Medical Imaging*. San Diego, CA, 2007
2. White RJ, Meoli DF, Swarthout RF, *et al*. Plexiform-like lesions and increased tissue factor expression in a rat model of severe pulmonary arterial hypertension. *Am J Physiol Lung Cell Mol Physiol*. 2007;293(3):L583–590. doi:10.1152/ajplung.00321.2006.
3. Hawkins A, Tulloh R. Treatment of pediatric pulmonary hypertension. *Vasc Health Risk Manag*. 2009;5:509–524.
4. Kheyfets VO, O'Dell W, Smith T, Reilly JJ, Finol EA. Considerations for Numerical Modeling of the Pulmonary Circulation—A Review With a Focus on Pulmonary Hypertension. *J Biomech Eng*. 2013;135(6):061011–061011. doi:10.1115/1.4024141.
4. Kirbas C, Quek F. A Review of Vessel Extraction Techniques and Algorithms. *ACM Comput Surv*. 2004;36(2):81–121. doi:10.1145/1031120.1031121.

VI. ACKNOWLEDGEMENTS